Computers & Geosciences 160 (2022) 105028

Contents lists available at ScienceDirect

Computers and Geosciences

journal homepage: www.elsevier.com/locate/cageo

gTOOLS, an open-source MATLAB program for processing high precision, relative gravity data for time-lapse gravity monitoring

Maurizio Battaglia [a,b,*], Antonina Calahorrano-Di Patre [c], Ashton F. Flinders [d]

[a] U.S. Geological Survey, Volcano Disaster Assistance Program, PO Box 158, NASA Ames Research Center, Bldg. 19, 2nd Floor, Moffett Field, CA, 94035, USA
[b] Department of Earth Sciences, Sapienza – University of Rome, P.le A. Moro 5, 00185, Rome, Italy
[c] Department of Earth Sciences, Simon Fraser University, 8888 University Drive, Burnaby, BC, V5A 1S6, Canada
[d] U.S. Geological Survey, Hawaiian Volcano Observatory, 1266 Kamehameha Ave Suite A5, Hilo, HI, 96720, USA

ARTICLE INFO

Keywords:
Open-source
Time-lapse gravity
Temporal gravity
Gravity monitoring
MATLAB
Relative gravity
Cotopaxi

ABSTRACT

gTOOLS is an open-source software for the processing of relative gravity data. gTOOLS is available in MATLAB and as a compiled executable to be run under the free MATLAB Runtime Compiler. The software has been designed for time-lapse (temporal) gravity monitoring. Although programmed to read the Scintrex CG-5 and CG-6 gravimeters output data files, it can be easily modified to read data files from other gravimeters. The software binds together single-task processing modules within a very simple user interface that is based on one text file. Gravity processing involves three modules: (a) gravimeter calibration; (b) automatic processing of gravity data to find adjusted gravity differences; and (c) post processing of results. Each module is optional and runs independently from the others. Data processing includes (a) averaging out the measurements noise, and correction for solid Earth tides, and ocean loading, and residual instrumental drift, and (b) calculate the residual instrumental drift and gravity differences between the base station and monitoring sites, and their uncertainties, by a weighted least square analysis of the gravity data. The software allows the automatic processing of a gravity campaign spanning multiple days in a single run. The software is tested on gravity data from 2015 eruption at Cotopaxi volcano, Ecuador.

1. Introduction

Time-lapse gravimetry is extensively employed in the monitoring of subsurface fluid flow. Examples includes monitoring of volcanic unrest (Carbone et al., 2017), assessment of CO_2 sequestration (Appriou et al., 2020), and oil reservoirs exploitation (Krahenbuhl et al., 2011). The gravity changes associated with these applications can vary between a few and a few hundred microGal (e.g., Van Camp et al., 2017; 1 μGal = 10^{-8} ms^{-2}). Portable, relative gravimeters like the Scintrex CG-5 and CG-6 are commonly employed in these applications thanks to their compact shape, limited size/weight, and automated features. If selected in the interface of the instruments, field measurements (taken at 6 Hz sampling rate) can be corrected in real time for tilt, internal temperature, solid Earth tides, seismic noise, and instrumental drift to obtain a gravity measurement and its standard deviation. The manufacturer specifies a nominal repeatability of 5 μGal for the CG-5 and less than 5 μGal for the CG-6 (Scintrex System, Operation Manual, 2014, 2018; Liu et al., 2019). Real-time corrections are useful to verify first-order results in the field, but post-processing is needed to achieve higher accuracy or for surveys where multiple gravimeters are used. Residual instrumental drift, the lack of correction for ocean loading and measurement noise from the field work itself (e.g., car transportation on dirt roads or rough terrains, or walking with the instrument in a backpack) can degrade the gravity measurements by some tens of μGal (Reudink et al., 2014) requiring more complete data corrections during post-processing to reach the desired precision.

gTOOLS is open-source software for the processing of relative gravity data. The software runs under Windows OS, but it can be modified to run under Linux or Mac OS. The software is available both in MATLAB and as a compiled executable to be run under the free MATLAB Runtime (https://www.mathworks.com/products/compiler/matlab-runtime.html). The software binds together single-task processing modules within a very simple user interface that is based on one text file (Fig. 1). The modular structure allows the software to be easily updated. The

* Corresponding author. U.S. Geological Survey, Volcano Disaster Assistance Program, PO Box 158, NASA Ames Research Center, Bldg. 19, 2nd floor, Moffett Field, CA, 94035, USA.
E-mail address: mbattaglia@usgs.gov (M. Battaglia).

https://doi.org/10.1016/j.cageo.2021.105028
Received 1 May 2021; Received in revised form 24 December 2021; Accepted 30 December 2021
Available online 7 January 2022

```
% File with folders, parameters and options controlling the automatic
% processing of gravity data from Scintrex CG5 or CG6
% parameter % comment
CG5                 % type of meter (CG5 or CG6)
./C578              % folder with raw gravity files [*.cvs]
C578                % gravity meter label0
0                   % earth tide correction [logic value: 1=yes 0=no]
1                   % ocean loading correction [logic value: 1=yes 0=no]
MSH_2016            % name for adjusted gravity file [output file]
```

Fig. 1. The input command file used to run the automatic processing of gravity measurements and the post processing of results. No input command file is needed to run the calibration module.

code allows for the speedy processing of raw gravity data from a network of gravity benchmarks composed of a base station and multiple monitoring sites. Data processing includes the removal of measurements noise, correction for solid Earth tides, ocean loading and residual instrumental drift. The residual instrumental drift, the relative gravity differences between the base station and monitoring sites, and associated errors, are estimated by a weighted least square analysis of the data set. The software allows the automatic processing of a gravity campaign spanning multiple days in a single run.

Earlier efforts to develop codes to reduce campaign gravity data, include CG3TOOLS (Gabalda et al., 2003), GravProcess (Cattin et al., 2015), and PyGrav (Hector and Hinderer, 2016). The first two programs

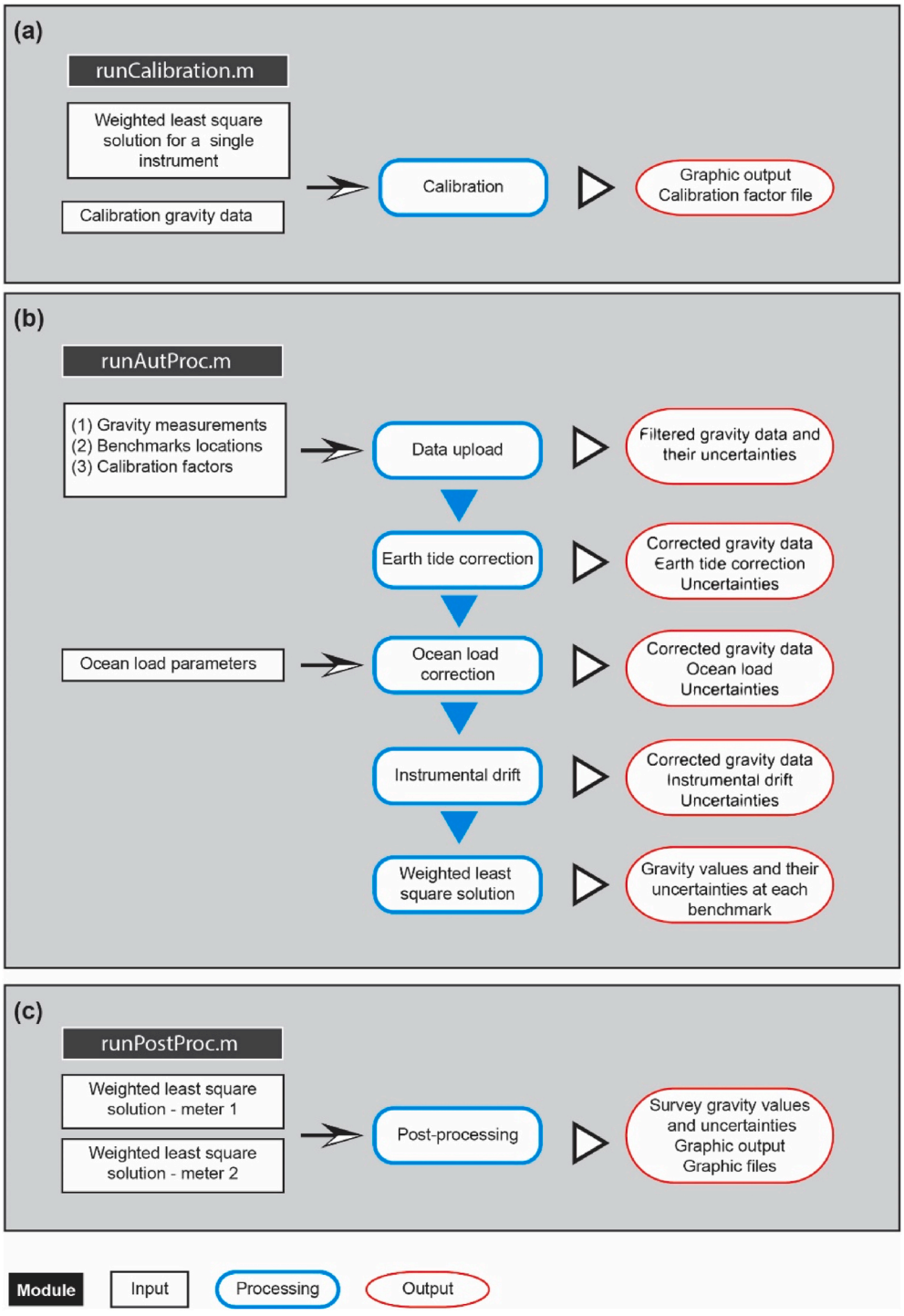

Fig. 2. Flow chart for gravity data processing, showing the three main modules of *gTOOLS*. Each module is optional and runs independently from the others. (a) *runCalibration.m* estimates the main calibration constant scale correction factor of a gravity meter (Scintrex System, Operation Manual, 2014, 5–37). If measurements for more than one calibration line are available, the code will first compute a single calibration scale correction factor for all the lines and then a calibration scale correction factor for each line. (b) for each meter, *runAutProc.m* takes processing options and parameters; reads the raw gravity data files; computes solid Earth tides [optional], computes the ocean loading [optional], models the residual instrumental drift, and calculates the weighted least square gravity values. (c) *runPostProc.m* takes the results from the gravity adjustment run (*runAutProc.m*) of two gravimeters; estimates and plots the scatter of the adjusted gravity measurements, and prints a text file with the mean adjusted gravity of the survey. Black boxes: *gTOOLS* module; white box: input files; cyan boxes: data processing; red boxes: output files. (For interpretation of the references to colour in this figure legend, the reader is referred to the Web version of this article.)

are coded in MATLAB, the third in Python. Data reduction, analysis, and representation in GravProcess (Cattin et al., 2015), and PyGrav, Hector and Hinderer (2016), are implemented by a graphical user interface. GravProcess (Cattin et al., 2015) implements free-air and terrain corrections as well. Recently, Kennedy (2020) released GSadjust. This software is a graphical user interface (GUI), built on PyGrav (Hector and Hinderer, 2016), that offers several plotting and analysis tools to correct, adjust and integrate relative and absolute campaign gravity data. All software employs similar reduction and analysis algorithms. The major differences between gTOOLS and the other software are: (a) gTOOLS is specifically designed for time lapse (temporal) gravity monitoring; (b) we spent significant efforts rigorously testing and verifying the code; (c) gTOOLS can be run by editing a single text command file and (d) The software allows the automatic processing of a gravity campaign spanning multiple days in a single run.

Here, we first introduce the general characteristics of the program (Section 2), then we present the calibration module (Section 3). Corrections for solid Earth tides (*ET*), ocean loading (*OL*) and residual instrumental drift (*RD*), and the weighted least-square system solved to obtain adjusted gravity measurements and their uncertainties are introduced in Section 4. The post-processing module is reviewed in Section 5. Because of the complexity of the development of gTOOLS, testing the software to detect existing logical or mathematical bugs is indispensable. We show the results of four dynamic tests in Section 6. Finally, we present the case study of time-lapse gravity monitoring of the unrest at Cotopaxi volcano, Ecuador (Section 7).

2. Gravity reduction

Gravity measurements processing in gTOOLS comprises three main modules: (1) gravimeter calibration; (2) automatic processing of gravity data to find adjusted gravity differences with a base station; and (3) post processing of results. Each module is optional and runs independently from the others. The different processing steps (shown in Fig. 2) are controlled by a single input text file (Fig. 1). These steps are performed by individual subroutines called by the main program modules.

gTOOLS requires two input data files:

1. a calibration file, with the gravimeter(s) constant scale correction factor *k*.
2. gravity data files (CSV format text file) in the Scintrex CG-5 or CG-6 format for each gravity meter and day of field work.

In the Scintrex acquisition data mode, unprocessed 6 Hz data (gravity, tilt-x, tilt-y, and temperature) are stored in memory. The built-in software can average the readings over a specific time interval, subtract the solid Earth tides from the data and correct the data for a linear drift. Gravity data can be dumped from the gravity meter to a PC using the Scintrex Data logger software, a serial dump program that can be used to export data as text files with the columns in the following order LATITUDE, LONGITUDE, ALTITUDE., TIDE CORRECTED GRAVITY, ST DEV, TILTX, TILTY, TEMPERATURE, EARTH TIDE, DURATION, MEASUREMENTS REJECTED, TIME, DEC. TIME + DATE, TERRAIN CORRECTION, DATE. Examples of input and output file formats are available in the gTOOLS software release.

Relative gravity values at gravity benchmarks can be described by the equation (Fig. 3):

$$k \cdot \hat{g}(t) = g(t) - ET(t) - OL(t) + RD(t) + \varepsilon \tag{1}$$

where t is the time of the measurement, $k{\cdot}\hat{g}(t)$ is the gravity reading, $\hat{g}$ the nominal instrument measurement, and K the scale correction factor (Scintrex System, Operation Manual, 2014, 5–37). $g(t)$ is the adjusted gravity value – the gravity value of interest for monitoring applications, $ET(t)$ the solid Earth tide correction, $OL(t)$ the ocean loading correction; $RD(t)$ the residual instrumental drift, and ε the residual instrumental/operator/site noise (Fig. 3). If the uncertainty for the scale correction factor (σ_k) and the residual instrumental/operator/site noise (ε) are such that $\sigma_k \sim \varepsilon < \sigma_g$, where σ_g is the uncertainty of the adjusted gravity value $g(t)$, then $g(t)$ and σ_g are given by the equation:

$$\begin{aligned} g(t) &\simeq k{\cdot}\hat{g}(t) + ET(t) + OL(t) - RD(t) \\ \sigma_g &\simeq \sqrt{k^2{\cdot}\sigma_{\hat{g}}^2 + \sigma_{ET}^2 + \sigma_{OL}^2 + \sigma_{RD}^2} \end{aligned} \tag{2}$$

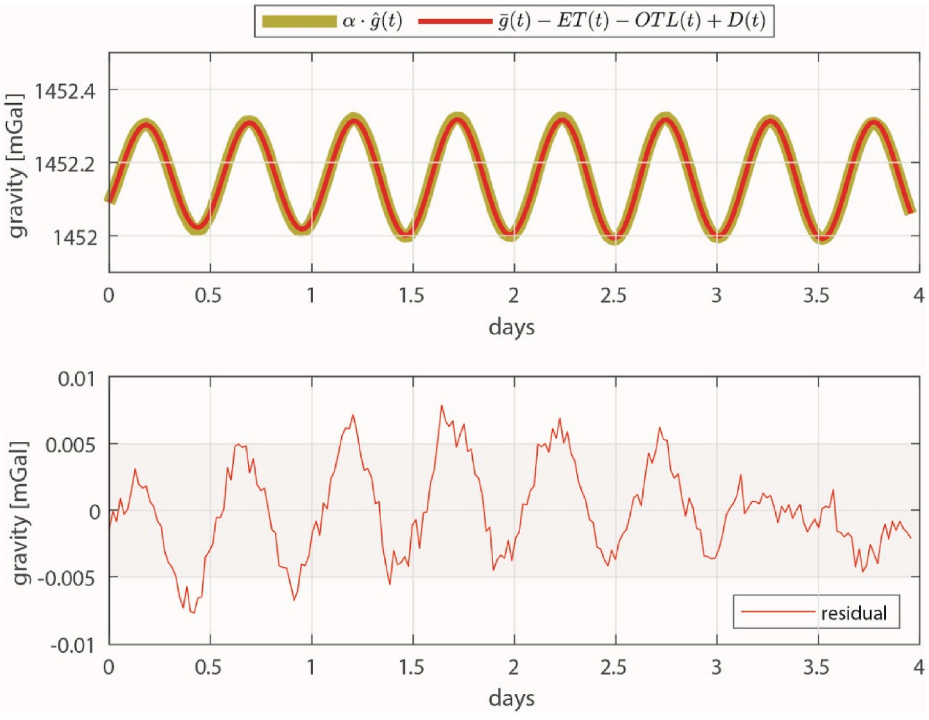

Fig. 3. Verification of equation (1). (Top) Gravity signal recorded for 4 days at site OTAVALO (Ecuador, Lat: 0.2376°, Long: −78.4560°, Elevation 3398 m a.s.l.) by Scintrex gravity meter CG-5877 (thick green line, $\alpha{\cdot}\hat{g}(t)$), compared against the model from (1) (thick red line, $g(t) - ET(t) - OL(t) + RD(t)$). (Bottom) Residual instrumental/operator/site noise ε from the fit of the observation data with the model. The residual is within the nominal repeatability (standard deviation) of 5 μGal for the CG-5 reported by the manufacturer (Scintrex System, Operation Manual, 2014). Data from OTAVALO are a courtesy of Mario Ruiz (IG-EPN, Ecuador). Some residual signal (less than 3 μGal), probably instrument noise, is not explained by the model. (For interpretation of the references to colour in this figure legend, the reader is referred to the Web version of this article.)

3. Gravity meter calibration

The U.S. Geological Survey checks the calibrations of gravity meters by measuring mountain gravity loops (calibration lines) in Mauna Loa (HI), Mt Hood (OR) and Mt Hamilton (CA); see Battaglia et al. (2018). Mountain gravity loops allow comparison of the gravity changes measured by an instrument against know gravity measurements over a large range of gravity values. The occupation of calibration lines provides at small cost information about changes in time and non-linearity of the calibration factor, unusual drift behavior and other instrument defects.

Scintrex gravity meters have a linear response between spring acceleration and gravity, so that the relation between nominal instrument readings and actual gravity values can be represented by a single calibration constant *GCAL1*. Scintrex calibrates the instrument with a relative precision of 0.01%, equivalent to an error of 0.01 mGal (10 μGal) in 100 mGal. To decrease the error to 0.001 mGal (1 μGal) in 100 mGal, equivalent to a relative error of 0.001%, users must estimate a scale correction factor of the main calibration constant *GCAL1* with a relative error of 10^{-5} (Scintrex, 2014, p. 5–37; (Valiant, 1991)see also Battaglia et al., 2018).

For this reason, we consider the manufacturer's calibration (i.e., *GCAL1* in the case of a Scintrex CG-5 or CG-6) as an approximation of the calibration constant. The scale correction factor (k) simulates the divergence from this approximation and must be estimated by the operator. We model the linear response of the gravity meter (Fig. 4) as

$$CALGRAVITY = intercept + k \times LSGRAVITY \quad (3)$$

The slope of the straight-line model above is the scale correction factor k; the intercept represents eventual systematic errors in the gravity measurements. If the uncertainties associated with the gravity measurements *LSGRAVITY* are much smaller than the errors associated with the calibration gravity measurements *CALGRAVITY*, then the slope and intercept of the straight-line model can be found solving a linear regression problem (Press et al., 1992, equation 15.2.6) – Fig. 4 (left). When the order of magnitude of the uncertainties of *LSGRAVITY* and *CALGRAVITY* can be compared then the slope and intercept of the straight-line model can be found by solving a non-linear regression problem (Press et al., 1992, equation 15.3.2) – Fig. 4 (right).

4. Processing

Adjustments to the field gravity measurements (solid Earth tides and ocean loading, the correction for the residual instrumental drift, weighted least square solution) are applied to measurements from each gravity meter by the module *runAutProc.m* (Fig. 2).

Although designed to process gravity data from a double occupation of a gravity network (the so-called double loop; see Chapter 7), the software can process data from a single loop as well.

4.1. Filter

Most gravimeters display a stabilization period, i.e., a non-linear evolution of the gravity value until it becomes stable. This stabilization period can last from a few minutes to tens of minutes, depending on the environmental noise and time and type of transportation between gravity sites. Once the gravimeter is stable, the occupation time and the read time should be programmed considering the balance between a read time short enough to give many readings and an occupation time long enough to give stable mean values (see section 7).

As a first step, the code reads gravity measurements (*gravity*), adjusts the measurements by the main calibration constant's scale correction factor $_k$ and computes the weighted mean (*GRAVITY*) and standard deviation (*SIGMA*) of gravity readings at each gravity benchmark. The weights represent the reciprocal of the root mean square errors from the CG-5 (or CG-6) output files. Measurements that fall outside of one *SIGMA* from the weighted mean *GRAVITY* are discarded.

Results of this initial filtering are plotted for all the sites to help identify unstable readings, or outliers (Fig. 5). The code allows to manually discard any reading that might be considered unstable, or an outlier, by commenting the appropriate line in the text data file.

4.2. Solid earth tides and ocean loading correction

These corrections are performed for each measurement using its specific location and time stamp. Scintrex follows the approach proposed by Longman (1959) to correct for solid Earth tides. We use the same approach but extend it to also a) compute the Moon and Sun longitudes with the original equations by Bartels (1957, p. 747), b) employ updated values from USNO (2011) for the astronomical constants and c) consider anelastic effects on tides (Agnew, 2007) - see Fig. 6.

The ocean loading correction *OTL*(t) module calls the Fortran code HARDISP by Petit and Luzum (2010) to compute the effect of ocean loading on local gravity (Fig. 7). Ocean loading coefficients in the example included with the code are from the TOPEX9.2a model (Egbert and Erofeeva, 2002). However, users can provide coefficients from any model they prefer. The ocean loading coefficients implemented in gTOOLS are from the Bos and Scherneck's ocean loading provider (available on-line at http://holt.oso.chalmers.se/loading/).

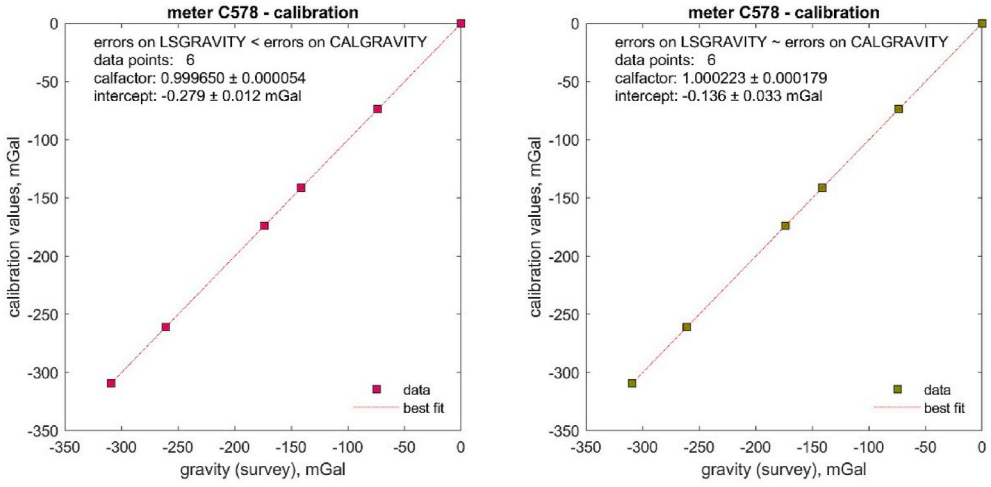

Fig. 4. Plots of the best fit to the linear response of a gravity meter, equation (3). Mt Hamilton USGS calibration line. The error of the scale correction factor (*calfactor*) shown on the plots is the standard error. (left) If the uncertainties associated with the gravity measurements *gravity (survey)* are much smaller than the errors associated with the *calibration values*, then the slope and intercept of the straight-line model can be found solving a linear regression problem (Press et al., 1992, 15.2). (right) When uncertainties of *gravity (survey)* and *calibration values* can be compared then the slope and intercept of the straight-line model can be found solving a non-linear regression problem (Press et al., 1992, 15.3). Note the different values for the slope (scale correction factor) of the two calibrations; the estimate of the scale correction factors may not be unique.

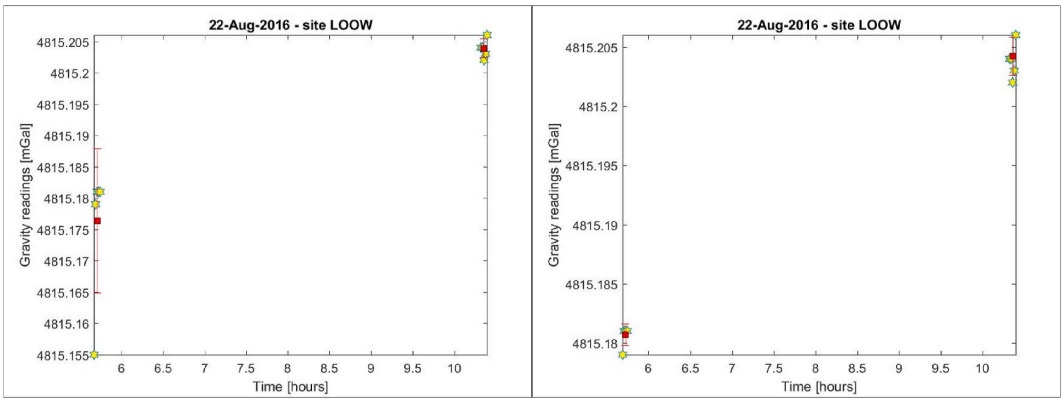

Fig. 5. Automatic data filtering in gTOOLS. Data have been collected with an occupation time of 5 min and a reading time of 1 min, after the meter became stable. (left) Unfiltered gravity data, showing five readings for each occupation of the site LOOW (Mount St. Helens). (right) Filtered gravity data, the code discarded one reading in the first occupation of LOOW (Mount St. Helens) because too noisy.

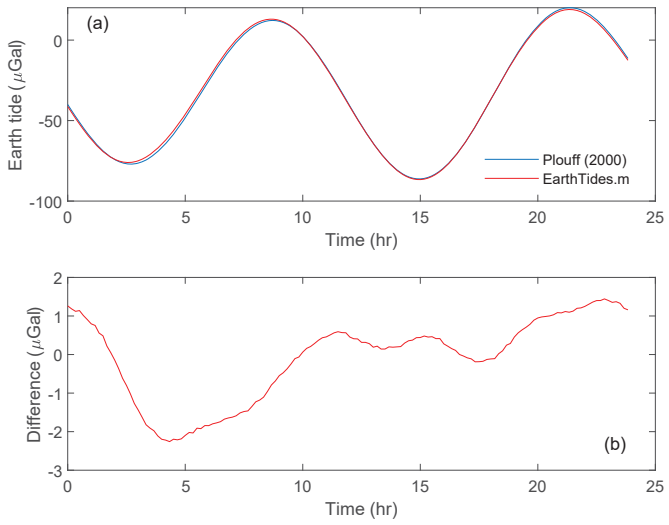

Fig. 6. Verification of the Earth tide module. Test site parameters, lat: 51°, long: −141°, elevation: 0 m a.s.l., date: 02-24-2012, GMT offset: 0 h. (a) Plot of the Earth tides from *tideg* by Plouff (2000) and the MATLAB script *EarthTides.m*; (b) Difference between the numerical outputs from the two codes.

4.3. Linear instrumental drift correction

In a time-lapse gravity survey, a double loop with two instruments is ideal and recommended (e.g., Jachens et al., 1981; Battaglia et al., 2008; Carbone et al., 2017). Every benchmark of the monitoring network is measured with at least two gravimeters during two complete loops through the network per day, with the base station remeasured three times.

To estimate the daily, linear instrumental drift parameters, the code first removes the average gravity value $\bar{g}$ from each benchmark, so that all the occupations are centered around zero (Fig. 8). The average value $\bar{g}$ is the solution of the weighted least square system

$$\bar{g}_i = \left[S_{ik} W_{kj} S_{ji}\right]^{-1} S_{ik} W_{kj} \tilde{g}_j \qquad \begin{matrix} i = 1, \ldots, N \\ j, k = 1, \ldots, M \end{matrix} \tag{4}$$

$$\bar{g}_i = \begin{bmatrix} \bar{g}_0 \\ \bar{g}_1 \\ \vdots \\ \vdots \\ \bar{g}_N \end{bmatrix} \begin{matrix} base \\ site_1 \\ \vdots \\ \vdots \\ site_N \end{matrix}, \quad S_{ij} = \begin{bmatrix} 1 & 1 & 1 & 0 & 0 & \cdots & \cdots & 0 \\ 0 & 0 & 0 & 1 & 1 & \cdots & \cdots & 0 \\ \vdots & & & & & \ddots & & \vdots \\ \vdots & & & & & & \ddots & \vdots \\ 0 & 0 & 0 & 0 & 0 & 0 & 1 & 1 \end{bmatrix}, \tag{5}$$

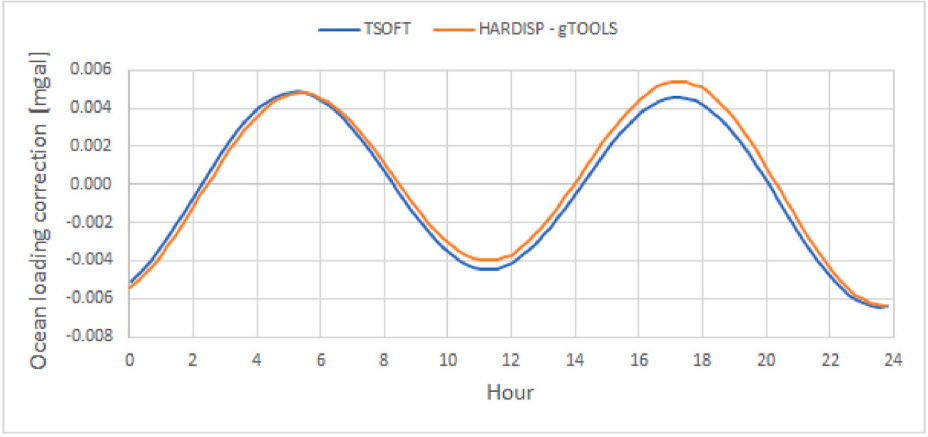

Fig. 7. Ocean loading correction from gTOOLS verified against the synthetic tide routine of TSOFT (Van Camp and Vauterin, 2005) for 24 h on 8/22/2016 at site 5040, Mount St Helens (Lat: 46.3695°, Long: −122.5819°, Elev: 253 m a.s.l.).

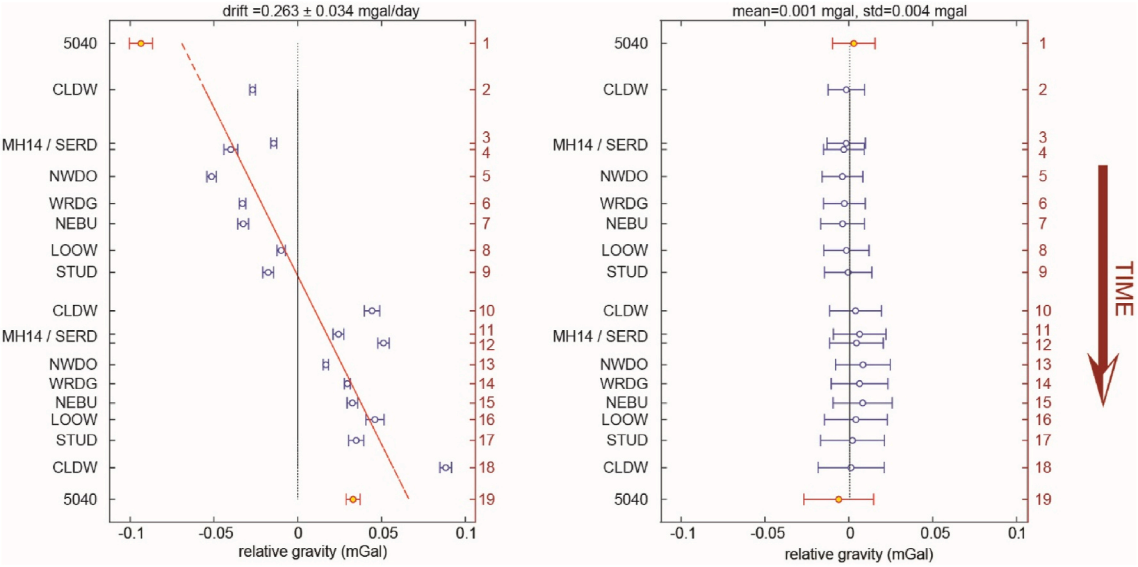

Fig. 8. Example of the residual instrumental drift correction from the gravity monitoring network of Mount St Helens (Battaglia et al., 2018) – survey date 08/22/2016. (left) Plot of $\widetilde{g}_j - \Pi_{j,i}\overline{g}$, equations (7) and (8). The MATLAB script *EarthTides.m* removes the average from each benchmark, so that all the occupations are centered around 0. A linear fit (red line) is then calculated through all points, collectively, at once. The number of benchmarks is $N = 7$, the number of benchmark occupations is $M = 19$. (right) Plot of the adjusted relative gravity measurements g_j for each benchmark occupation, equation (2), after the residual instrumental drift $RD_j = p_{1,1}t_j + p_{1,2}$ has been removed from $\widetilde{g}_j$. (For interpretation of the references to colour in this figure legend, the reader is referred to the Web version of this article.)

$$W_{kj} = \begin{bmatrix} w_1^0 & & & & & & & \\ & w_2^0 & & & & & & \\ & & w_3^0 & & & & & \\ & & & w_1^1 & & & & \\ & & & & w_2^1 & & & \\ & & & & & \ddots & & \\ & & & & & & w_1^N & \\ & & & & & & & w_2^N \end{bmatrix}, \quad \widetilde{g}_j = \begin{bmatrix} \widetilde{g}_1^0 & base_1 \\ \widetilde{g}_2^0 & base_2 \\ \widetilde{g}_3^0 & base_3 \\ \widetilde{g}_1^1 & site_1^1 \\ \widetilde{g}_2^1 & site_2^1 \\ \vdots & \vdots \\ \widetilde{g}_1^N & site_1^N \\ \widetilde{g}_2^N & site_2^N \end{bmatrix}, \tag{6}$$

where $\widetilde{g}_j \simeq k\cdot\widehat{g}_j + ET_j + OL_j$ and $\widetilde{\sigma}_j \simeq \sqrt{k^2\cdot(\sigma_g^j)^2 + (\sigma_{ET}^j)^2 + (\sigma_{OL}^j)^2}$ are the gravity measurements at each benchmark and their errors, S_{ij} is a sparse matrix describing the benchmark occupations, W_{kj} is the diagonal matrix of weights $w_j = 1/\widetilde{\sigma}_j^2$, N is the number of benchmarks, and M the number of gravity measurements (or benchmark occupations) with $N < M$.

Once the average value is removed from all gravity measurements, the residual instrumental drift (Fig. 7) is given by the least square solution

$$p_{1-2,1} = \left[M_{1-2,j}M_{j,1-2}\right]^{-1}\left[\widetilde{g}_j - \Pi_{j,i}\overline{g}_i\right] \tag{7}$$

where $M_{j,1-2}$ is a rectangular matrix whose first column is the time t_j of the measurement and the second column is the unit vector, $p_{1,1-2}$ is a column vector whose first element is the instrumental drift rate and the second element models the instrument noise

$$\widetilde{g}_j - \Pi_{j,i}\overline{g} = \begin{bmatrix} \widetilde{g}_1^0 - \overline{g}_0 \\ \widetilde{g}_2^0 - \overline{g}_0 \\ \widetilde{g}_3^0 - \overline{g}_0 \\ \widetilde{g}_1^1 - \overline{g}_1 \\ \widetilde{g}_2^1 - \overline{g}_1 \\ \vdots \\ \widetilde{g}_1^N - \overline{g}_N \\ \widetilde{g}_2^N - \overline{g}_N \end{bmatrix} \quad M_{j,1-2} = \begin{bmatrix} t_1 & 1 \\ t_2 & 1 \\ t_4 & 1 \\ t_4 & 1 \\ t_5 & 1 \\ \vdots & \vdots \\ t_{M-1} & 1 \\ t_M & 1 \end{bmatrix} \tag{8}$$

GravProcess (Cattin et al., 2015) and PyGrav (Hector and Hinderer, 2016) employ a similar approach to eliminate the linear instrumental drift, i.e., the drift is estimated by a least-square fit of the weighted time series. DSAdjust (Kennedy, 2020) implements four different reduction schemes.

4.4. Mean gravity measurements

The final adjusted relative gravity values Δg_i is the solution of the weighted least square inversion

$$\Delta g_i = \left[S_{ik}W_{kj}S_{ji}\right]^{-1}S_{ik}W_{kj}\left(g_j - g_0\right) \quad \begin{matrix} i = 1,\ldots,N \\ j,k = 1,\ldots,M \end{matrix} \tag{9}$$

where S_{ij} is the sparse matrix from equation (5), W_{kj} is the diagonal matrix of weights $w_j = 1/\sigma_j^2$, g_j and σ_j are is adjusted gravity from equation (2), and g_0 is the average adjusted value at the base station. According to Gurland and Tripathi (1971), the errors σ_i can be estimated using the unbiased standard deviation

$$\sigma_i = s_i\left[1 + \frac{0.25}{N_s - 1}\right], \quad s_i = \sqrt{\chi_v^2\Sigma_{ii}}, \quad \begin{matrix} N_s = 3 & base \\ N_s = 2 & site \end{matrix} \tag{10}$$

The chi-square per degree of freedom χ_v^2 and the covariance matrix

Σ_{ij} are given by the solution of (9).

5. Post processing

The *runPostProc.m* module takes the results from the previous gravity adjustment procedure (see section 4) to estimate the average adjusted relative gravity value Δg_i at each benchmark for the survey and plot the scatter of the adjusted gravity measurements Δg_i at each site, including uncertainties – see Fig. 9.

6. Software verification and limitations

6.1. Verification

Due to the complexity of the mathematical models involved in the development and operation of gTOOLS, testing the software to detect existing subtle faults is critical (Farrell et al., 2011). We run four dynamic tests to verify the code:

1. we verified the Earth Tide correction (*EarthTide.m*) against the FORTRAN 77 routine *tideg* by Plouff (2000) – Fig. 6.
2. we verified the Ocean Loading correction (*OCVLoading.m*) against the synthetic tide routine of TSOFT (Van Camp and Vauterin, 2005) – Fig. 7.
3. we verified the theoretical model in (1) against experimental data (Fig. 3).
4. we verified the algorithm of the gravity adjustment module, *runAutProc.m*, using a synthetic data set based on equation (1), and the time stamps and benchmark locations of the 2016 survey of the gravity monitoring network of Mount St Helens (WA; Battaglia et al., 2018) – Fig. 9.
5. finally, we tested the entire code against GSadjust (Kennedy, 2020) and PyGrav (Hector and Hinderer, 2016) – Table 1.

6.2. Limitations

The present version of the software has one significant computational disadvantage compared to other software. The ocean loading correction employs the compiled version of the HARDISP Fortran code by Petit and Luzum (2010). The compiled version of HARDISP depends on the operating system. The version available in gTOOLS has been compiled under Windows and will not run under MacOS or Linux.

Table 1
Comparison of the adjusted gravity values for the August 22, 2016, survey at Mt. St. Helens (Battaglia et al., 2018). Adjusted values estimated using GSadjust/-PyGrav and gTOOLS. The raw gravity values have been corrected for measurement noise, ocean loading and linear instrument drift. Final adjusted values have been computed by weighted least squares.

SITE	Gsadjust/PyGrav		gTOOLS		difference
	gravity	st dev	gravity	st dev	
	[mGal]	[mGal]	[mGal]	[mGal]	[mGal]
5040	0.000	0.001	0.003	0.014	0.003
CLDW	−185.531	0.002	−185.522	0.010	0.009
LOOW	−308.146	0.002	−308.149	0.015	−0.003
MH14	−488.435	0.002	−488.432	0.013	0.003
NEBU	−317.673	0.002	−317.676	0.015	−0.003
NWDO	−466.951	0.002	−466.956	0.014	−0.005
SERD	−488.009	0.002	−488.006	0.013	0.003
STUD	−236.158	0.002	−236.157	0.016	0.001
WRDG	−455.518	0.002	−455.522	0.014	−0.004

GravProcess (Cattin et al., 2015) and PyGrav (Hector and Hinderer, 2016) employ translations into MATLAB (or Python) of the SPOTL code (Agnew, 2012).

gTOOLS, GravProcess (Cattin et al., 2015) and PyGrav (Hector and Hinderer, 2016) only eliminate the linear instrument drift, while DSAdjust (Kennedy, 2020) uses four different reduction schemes.

7. Gravity monitoring of Cotopaxi volcano

Regarded as one of the most dangerous volcanic systems in Latin America, the monitoring of Cotopaxi volcano is done by the Instituto Geofisico de la Escuela Politecnica Nacional (IG-EPN) using infrasound, seismic and geodetic monitoring networks (Bernard et al., 2016; Gaunt et al., 2016; Hidalgo et al., 2016; Mothes et al., 2017). Cotopaxi experienced a new period of heightened activity in April 2015, which peaked during the eruptive activity of August 14, 2015 (Mothes et al., 2017). Summit ash emissions continued until November 2015. Monitoring parameters decreased until they returned to background levels in March 2016 (Hidalgo et al., 2018). Although several plausible sources for the unrest were inferred from modelling of monitoring data (Bernard et al., 2016; Morales Rivera et al., 2017; Hidalgo et al., 2018), and from petrological analysis (e.g., Gaunt et al., 2016; Troncoso et al., 2017), these techniques did not uniquely constrain sub-surface mass change. To

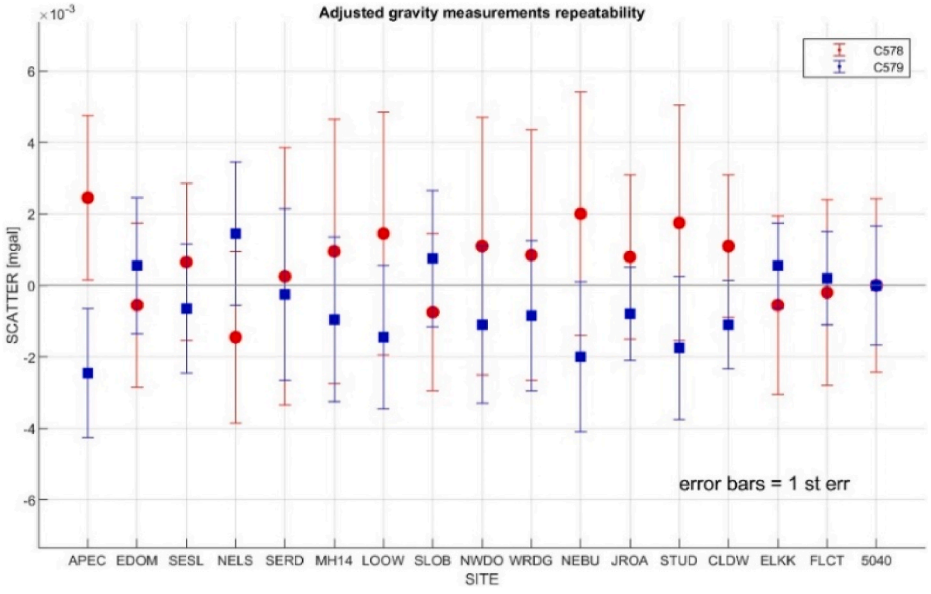

Fig. 9. Plot of the scatter of the adjusted gravity measurements recovered by the processing module (*runAutProc.m*). The synthetic gravity model of the 2016 gravity survey at Mount St Helens (Battaglia et al., 2018) is an ideal model to test the correct operation of the software. If the software correctly removes the different synthetic effects and instrumental noise, the scatter of the relative average adjusted gravity Δg_i should be negligible. The model includes solid Earth tide and ocean loading effects, linear residual instrumental drift, free-air effect, and residual gravity from a spherical model. The two instruments are differentiated through their scale correction factor, equation (1). White noise is added to simulate additional sources of uncertainties. The scattering is less than 5 μGal – within the nominal repeatability of 5 μGal for the CG-5 and less than 5 μGal for the CG-6 (Scintrex System, Operation Manual, 2014).

constrain sub-surface mass movements, an initial plan for time-lapse gravity monitoring was implemented at Cotopaxi by installing 3 survey stations in June 2015. The gravity network was expanded in October 2015 with the addition of 5 survey stations and an additional far-off base station (site OVC; Fig. 10). Gravity measurements were performed bi-monthly during the heightened activity, while the frequency of measurements was decreased after the end of unrest in March 2016 (Calahorrano-Di Patre et al., 2019).

Surveys at Cotopaxi were performed using a single CG-5 Scintrex relative gravimeter. Survey day loops were designed using the so-called "step method" (Greco et al., 2012), where two or more stations, including the base station, were repeated at least twice in a day (e.g., stat1 → stat2 → stat3 → stat2 → stat1). To minimize the possibility of including data with systematic instrumental errors, several identical loops were repeated in one survey and considered independent from each other. The change between gravity differences in one survey was considered the final measurement error. Other environmental effects (such as pressure changes and temperature) were monitored during data collection. These effects were also minimized with the placement of an insulating foam box around the gravity meter during measurements along with the use of a strong portable windbreak. Finally, since the travel time between stations at Cotopaxi is relatively long (typically more than 2 h), it was not unusual to observe a hysteresis effect (intrinsic to the Scintrex CG-5, e.g., Klees et al., 2017; Seigel, 1995) in the gravity data. Therefore, at least 20 min of stabilization time (measurements not considered as valid in the final mean) were required for each hour of careful transport, after which an additional 15-min period of valid measurements were collected to detect any lingering relaxation or data tares.

Until July 2018, a total of 16 surveys were completed at Cotopaxi volcano. Data from these surveys were corrected and processed in its entirety using gTOOLS. Basic corrections to gravity data included removing tidal effects, filtering outliers, and calculating and reducing the daily instrumental drift. The final error for the calculated gravity differences was estimated using the standard deviation in the data, the residuals from the drift calculation, and the repeatability for each survey. Although normally time-lapse gravity data is corrected for height changes in each station due to ground displacement, the free-air gravity effect caused by inflation at Cotopaxi did not surpass instrumental error, and thus is not considered for the calculation of residual gravity. An example of data reduction step by step is presented in Table 2 and Table 3. The results from the gTOOLS processing are visualized in Fig. 11, with station CAME as reference for the period before October 2015, and station OVC as reference after its installation in October 2015.

Two periods of gravity change, coinciding with volcanic activity, are shown in Fig. 10, notably June–August 2015 (pre-eruption) and October 2015–March 2016 (post-eruption). Although gravity changes are also observed in periods of inactivity (e.g., January–September 2017), the rate of change is not comparable to that observed during and immediately after eruptive activity. For example, during the period of Oct 2015 to March 2016, a gravity decrease was observed in almost all measured sites except REF, with the largest change observed at station VC1 of −72 μGal. During the period of January–September 2017, a gravity decrease was again observed at several stations at Cotopaxi (Fig. 10), with the largest change in this period of −35 μGal at station VC1. Therefore, the maximum rate of change was more than double during periods of volcanic unrest (~15 μGal/month) in comparison with periods of relative volcanic inactivity (~5 μGal/month). Gravity changes from the period of October 2015–March 2016 were therefore interpreted as being related to volcanic activity and were inversely modelled to explore sub-surface mass movement post-eruptive activity. Because of a lack of coverage, it is not possible to invert model data collected before the eruptive activity and forward modelling of sources inferred from deformation data was inconclusive (Calahorrano-Di Patre et al., 2017). The post-eruptive gravity changes at Cotopaxi were inversely modelled using several magmatic sources, assuming both an increase and a decrease of sub-surface mass into the modelled source (Calahorrano-Di Patre et al., 2019). The best model contemplated the migration of hydrothermal fluids for a deeper annulus-like aquifer to a cylindrical shallow, perched aquifer (Fig. 12).

With the addition of the inverse modelling of the gravity data to the already existing information from geochemistry, petrology, and seismology we were able to propose a conceptual model for this phase of Cotopaxi's activity. (Fig. 12; Calahorrano-Di Patre et al., 2019): a A magma body (best modeled by a spheroidal source) intruded approx. 12 km b.s.l. and triggered the measured pre-eruptive deformation and seismicity. b) A smaller source of magma, inferred from SO_2 and petrological data, ascended from a deeper reservoir and intermingled with the hydrothermal system, starting the eruptive activity. c) Hydrothermal fluids moved upwards from a deeper aquifer to a shallower level of the aquifer because of the source's heat, and this mass movement was detected by gravity measurements. d) A new equilibrium was reached, and all geophysical signals returned to background levels (e.g., SO_2 and seismicity), or stabilized at a new level (e.g., deformation and gravity).

8. Summary and conclusions

A fast, easy to use and reliable program for processing gravity data is a valuable tool for volcano observatories and scientists since time-lapse gravity monitoring of active volcanoes provides information on sub-surface mass change in times of unrest. For example, gravity data from the unrest of Cotopaxi (Ecuador), Yellowstone (WY) and Laguna

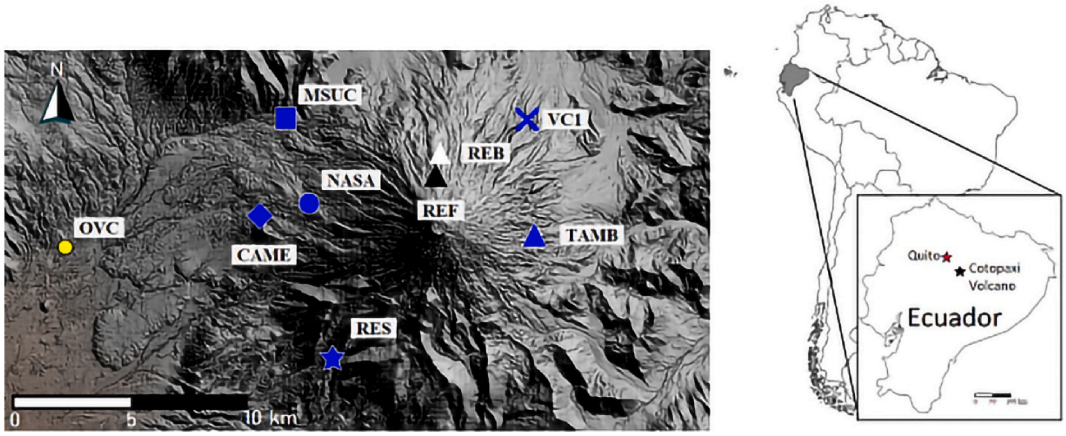

Fig. 10. Network of campaign gravity stations installed at Cotopaxi volcano between June 2015 and September 2016. Symbols for each station are the same as in Fig. 11. The location of Cotopaxi volcano relative to the capital city of Ecuador (Quito) can be seen on the right.

Table 2
Raw gravity data collected during one day loop at Cotopaxi volcano in January 2016 and processed with gTOOLS. The raw gravity (RGRAV) data, alongside its standard deviation (σ) are shown. We employed the gravity data corrected for the solid Earth tide by the software interface of the CG-5. FGRAV represents the averaged raw data after removal of outliers. TGRAV is the gravity data after the ocean loading effect has been removed, and DGRAV is the result after the daily drift correction has been applied. The last column shows the standard deviation calculated by considering both the individual error carried from the raw data, as well as the deviation of the calculated drift from the linear estimation of each of the station data.

Station	Date (dd-mmm-yy)	Time (UTC hh:mm:ss)	RGRAV (mGal)	σ (mGal)	FGRAV (mGal)	TGRAV (mGal)	DGRAV (mGal)	σ (mGal)
OVC	14-Jan-2016	13:59:09	1486.279	0.001	1486.279	1486.230	1486.243	0.003
CAME	14-Jan-2016	16:41:16	1385.713	0.004	1385.713	1385.712	1385.720	0.005
VC1	14-Jan-2016	20:03:01	1301.279	0.002	1301.279	1301.415	1301.417	0.004
CAME	14-Jan-2016	23:14:40	1385.654	0.005	1385.654	1385.730	1385.726	0.007
OVC	15-Jan-2016	01:09:06	1486.259	0.003	1486.259	1486.248	1486.240	0.005

Table 3
Summary of data from the January 2016 gravity survey at Cotopaxi volcano, as presented by gTOOLS at the end of the processing routine. LSGRAV refers to the difference between the measured relative gravity at the surveyed site and the value measured at the beginning of the loop at base station OVC. The standard deviation presented here reflects the repeatability of measurements at stations relative to the same day loop (and therefore, it was not calculated at stations that had only been measured once per day-loop). To compare gravity changes between surveys, these results and errors for each station must be merged into singular values per survey. LSGrav: least-square adjusted gravity; Std Dev: Standard Deviation; Std Err: standard error (see section 4.4).

Station	Date (dd-mmm-yy)	LSGrav (mGal)	Std Dev (mGal)	Std Err (mGal)
CAME	12-Jan-2016	−100.511	0.005	0.004
NAS	12-Jan-2016	−157.633	NaN	NaN
OVC	12-Jan-2016	−0.0004,	0.006	0.044
CAME	13-Jan-2016	−100.516	NaN	NaN
NAS	13-Jan-2016	−157.631	NaN	NaN
OVC	13-Jan-2016	0.0005,	0.002	0.001
CAME	14-Jan-2016	−100.518	0.003	0.002
OVC	14-Jan-2016	−0.0006,	0.004	0.003
VC1	14-Jan-2016	−184.824	NaN	NaN
CAME	15-Jan-2016	−100.510	0.003	0.002
MSUC	15-Jan-2016	−107.926	NaN	NaN
OVC	15-Jan-2016	−0.0004,	0.003	0.002
VC1	15-Jan-2016	−184.822	NaN	NaN
MSUC	16-Jan-2016	−107.931	NaN	NaN
OVC	16-Jan-2016	0.0000,	0.0006	0.0004
REFf	16-Jan-2016	−368.100	NaN	NaN

del Maule (Chile) have been processed in their entirety using the gTOOLS software. (Calahorrano-Di Patre et al., 2017; Poland and de Zeeuw-van Dalfsen, 2019; Trevino et al., 2021). Although designed for volcano observatories, the software can be readily employed in any field that monitors sub-surface mass flow.

The program reads input data files from Scintrex CG-5 and CG-6, but the input module can be easily modified to read data files from other gravimeters. Data processing includes the removal of measurement noise, and correction for residual instrumental drift, ocean loading and Earth tides. The code can process both single and double loop gravity surveys and allows the automatic processing of relative gravity data from a campaign spanning multiple days in a single run.

The main limitation of the present version of gTOOLS is that the ocean tide loading correction employs the compiled version of the HARDISP Fortran code by Petit and Luzum (2010). The version available in gTOOLS has been compiled under Windows and will not run under MacOS or Linux. Furthermore, the code corrects the effect of daily, linear instrument drift.

On the other hand, the software is open-source, stable, thoroughly verified and tested, and can be downloaded from a public repository managed by the US Geological Survey.

Computer code availability

- Name of code: gTOOLS
- developers and contact address
  - o Maurizio Battaglia, US Geological Survey, Volcano Disaster Assistance Program, PO Box 158, NASA Ames Research Center, Bldg. 19, 2nd floor, Moffett Field CA 94035. (650) 439–2629. mbattaglia@usgs.gov
  - o Ashton F. Flinders, US Geological Survey, Hawaiian Volcano Observatory, 1266 Kamehameha Ave Suite A5 Hilo HI 96720. aflinders@usgs.gov
- year first available: 2012
- hardware required: PC with 8 GB of RAM
- software required: MATLAB 2020a or higher to run the open-source code; the free MATLAB Compiler Runtime R2021a (9.10) - Windows OS 64-bit for the compiled code
- program language: MATLAB (R2021a)
- program size: 30 Mb

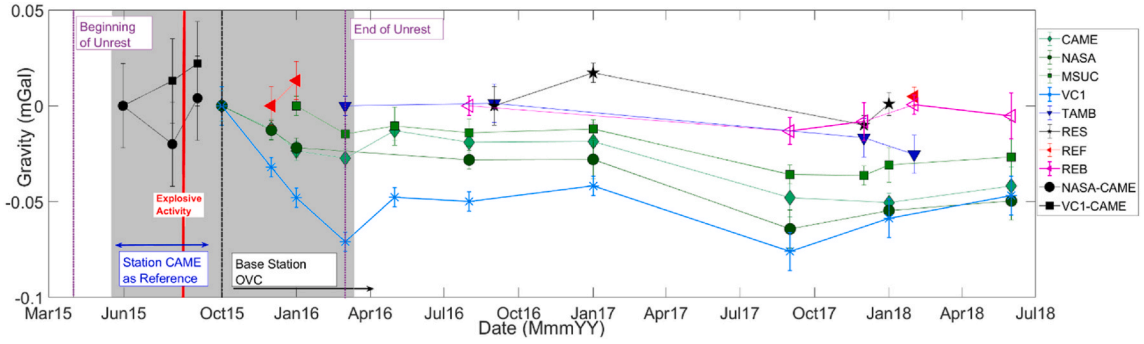

Fig. 11. Residual gravity measured at stations on Cotopaxi volcano from June 2015 to June 2018. The unrest and eruption period of 2015–2016 is shown between purple vertical lines. Modelled gravity data is shown in the grey shaded area. Gravity changes measured after the end of unrest are presented as a baseline for "normal" gravity variations at Cotopaxi: although the magnitude of changes might be comparable, the rate of gravity change during the unrest was undoubtedly accelerated. All gravity change is presented in comparison to the base station OVC, except for the three data points from June 2015 to September 2015. Modified after (Calahorrano-Di Patre et al., 2019). (For interpretation of the references to colour in this figure legend, the reader is referred to the Web version of this article.)

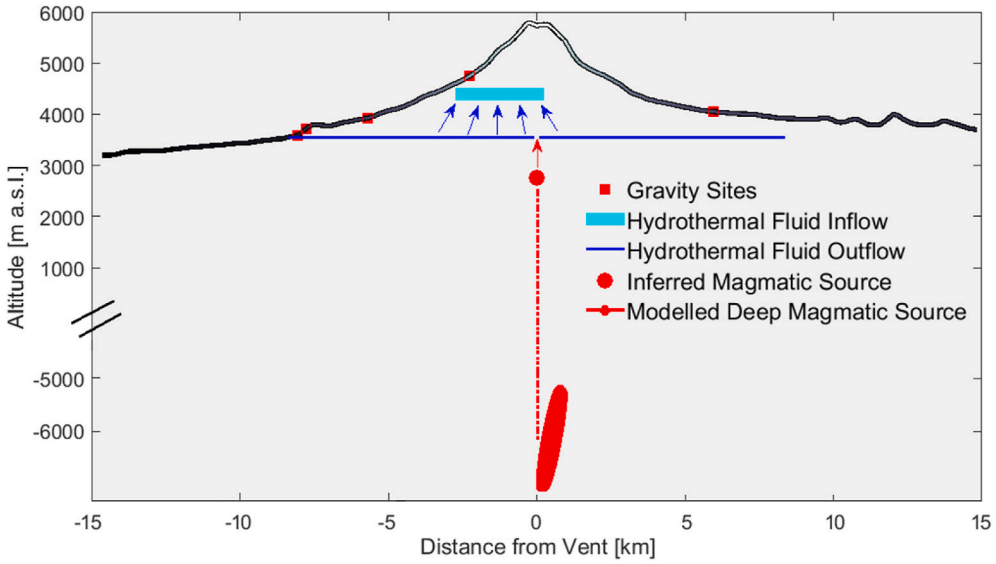

Fig. 12. Comprehensive model of Cotopaxi's period of unrest between 2015 and 2016 surmised from geophysical, geochemical, and petrological data. Modified after (Calahorrano-Di Patre et al., 2019).

- how to access the source code:
  → we waive copyright and related rights in the work worldwide through the CC0 1.0 Universal public domain dedication.
  → https://code.usgs.gov/vsc/publications/gtools

Link to the code

https://code.usgs.gov/vsc/publications/gtools.

Authorship statement

Maurizio Battaglia developed the code. Antonina Calahorrano-Di Patre applied gTOOLS to the gravity monitoring of the unrest at Cotopaxi volcano (Ecuador). Ashton F. Flinders verified the code and developed parts of the code. All the authors contributed equally in writing the manuscript.

Declaration of competing interest

The authors declare that they have no known competing financial interests or personal relationships that could have appeared to influence the work reported in this paper.

Acknowledgments

Comments by Mathijs Koymans (KNMI), Elske de Zeeuw-van Dalfsen (TU Delft), and one anonymous reviewer greatly helped to improve the manuscript. Funding for this work came from USAID via the Volcano Disaster Assistance Program and from the U.S. Geological Survey (USGS) Volcano Hazards Program. Any use of trade, firm, or product names is for descriptive purposes only and does not imply endorsement by the U.S. Government.

References

Agnew, D.C., 2007. Earth tides. In: Treatise on Geophysics: Geodesy. Elsevier, New York, pp. 163–195.
Agnew, D.C., 2012. SPOTL: Some Programs for Ocean-Tide Loading, SIO Technical Report. SIO. http://escholarship.org/uc/sio_techreport.
Appriou, D., Bonneville, A., Zhou, Q., Gasperikova, E., 2020. Time-lapse gravity monitoring of CO2 migration based on numerical modeling of a faulted storage complex. Int. J. Greenh. Gas Control 95, 102956. https://doi.org/10.1016/j.ijggc.2020.102956.
Battaglia, M., Gottsmann, J., Carbone, D., Fernández, J., 2008. 4D volcano gravimetry. Geophysics 73 (6), WA3–WA18. https://doi.org/10.1190/1.2977792.
Battaglia, M., Lisowski, M., Dzurisin, D., Poland, M.P., Schilling, S., Diefenbach, A., Wynn, J., 2018. Mass addition at Mount St. Helens, Washington, inferred from repeated gravity surveys. J. Geophys. Res. Solid Earth 123 (2), 1856–1874. https://doi.org/10.1002/2017JB014990.
Bartels, J., 1957. Gezeitenkräfte, Handbuch der Physik, XLVIII. Geophysik II, Springer-Verlag, Berlin, p. 1957.
Bernard, B., Battaglia, J., Proaño, A., Hidalgo, S., Vásconez, F., Hernandez, S., Ruiz, M., 2016. Relationship between volcanic ash fallouts and seismic tremor: quantitative assessment of the 2015 eruptive period at Cotopaxi volcano, Ecuador. Bull. Volcanol. 78 (11), 1–11. https://doi.org/10.1007/s00445-016-1077-5.
Calahorrano-Di Patre, A., Williams-Jones, G., Battaglia, M., Mothes, P., Gaunt, E., Zurek, J., Witter, J., 2019. Hydrothermal fluid migration due to interaction with shallow magma: insights from gravity changes before and after the 2015 eruption of Cotopaxi volcano, Ecuador. J. Volcanol. Geoth. Res. 387, 106667. https://doi.org/10.1016/j.jvolgeores.2019.106667.
Calahorrano-Di Patre, A., Williams-Jones, G., Battaglia, M., Mothes, P., Hidalgo, S., Aguaiza, S., Gaunt, H., 2017. Linking Gravity Change at Cotopaxi Volcano with the Volcanic Processes Responsible for the 2015-2016 Period of Unrest. *IAVCEI 2017*, vol. 150. Scientific Assembly, Portland.
Carbone, D., Poland, M.P., Diament, M., Greco, F., 2017. The added value of time-variable microgravimetry to the understanding of how volcanoes work. Earth Sci. Rev. 169, 146–179. https://doi.org/10.1016/j.earscirev.2017.04.014.
Cattin, R., Mazzotti, S., Baratin, L.M., 2015. GravProcess: an easy-to-use MATLAB software to process campaign gravity data and evaluate the associated uncertainties. Comput. Geosci. 81, 20–27. https://doi.org/10.1016/j.cageo.2015.04.005.
Egbert, G.D., Erofeeva, S.Y., 2002. Efficient inverse modeling of barotropic ocean tides. J. Atmos. Ocean. Technol. 19 (2), 183–204. https://doi.org/10.1175/1520-0426(2002)019<0183:EIMOBO>2.0.CO;2.
Farrell, P.E., Piggott, M.D., Gorman, G.J., Ham, D.A., Wilson, C.R., Bond, T.M., 2011. Automated continuous verification for numerical simulation. Geosci. Model Dev. (GMD) 4 (2), 435–449. https://doi.org/10.5194/gmd-4-435-201.
Gabalda, G., Bonvalot, S., Hipkin, R., 2003. CG3TOOL: an interactive computer program to process Scintrex CG-3/3M gravity data for high-resolution applications. Comput. Geosci. 29 (2), 155–171. https://doi.org/10.1016/S0098-3004(02)00114-0.
Gaunt, H.E., Bernard, B., Hidalgo, S., Proaño, A., Wright, H., Mothes, P., Kueppers, U., 2016. Juvenile magma recognition and eruptive dynamics inferred from the analysis of ash time series: the 2015 reawakening of Cotopaxi volcano. J. Volcanol. Geoth. Res. 328, 134–146. https://doi.org/10.1016/j.jvolgeores.2016.10.013.
Greco, F., Currenti, G., D'Agostino, G., Germak, A., Napoli, R., Pistorio, A., Del Negro, C., 2012. Combining relative and absolute gravity measurements to enhance volcano monitoring. Bull. Volcanol. 74 (7), 1745–1756. https://doi.org/10.1007/s00445-012-0630-0.
Gurland, J., Tripathi, R.C., 1971. A simple approximation for unbiased estimation of the standard deviation. Am. Statistician 25 (4), 30–32. https://doi.org/10.1080/00031305.1971.10477279.
Hector, B., Hinderer, J., 2016. pyGrav, a Python-based program for handling and processing relative gravity data. Comput. Geosci. 91, 90–97. https://doi.org/10.1016/j.cageo.2016.03.010.
Hidalgo, S., Battaglia, J., Arellano, S., Sierra, D., Bernard, B., Parra, R., Samaniego, P., 2018. Evolution of the 2015 Cotopaxi eruption revealed by combined geochemical and seismic observations. G-cubed 19 (7), 2087–2108. https://doi.org/10.1029/2018GC007514.

Hidalgo, S., Bernard, B., Battaglia, J., Gaunt, E., Barrington, C., Andrade, D., et al., 2016, April. Cotopaxi volcano's unrest and eruptive activity in 2015: mild awakening after 73 years of quiescence. In: EGU General Assembly Conference Abstracts, pp. EPSC2016–5043.

Jachens, R., Spydell, D., Pitts, G., Dzurisin, D., Roberts, C., 1981. In: Temporal Gravity Variations at Mount St. Helens, March-May 1980, The 1980 Eruptions of Mount. U.S. Geological Survey Professional Paper, vol. 1250. St. Helens, Washington, pp. 175–182. https://doi.org/10.3133/pp1250.

Kennedy, J., 2020. GSadjust v1.0. U.S. Geological Survey Software Release,, doi: 10.5066/P9YEIOU8..

Klees, R., Reudink, R.H.C., Flikweert, P.L.M., 2017. Tilt susceptibility of the Scintrex CG-5 autograv gravity meter revisited. In: International Association of Geodesy Symposia, vol. 12, pp. 119–123. https://doi.org/10.1007/1345_2017_4.

Krahenbuhl, R.A., Li, Y., Davis, T., 2011. Understanding the applications and limitations of time-lapse gravity for reservoir monitoring. Lead. Edge 30 (9), 1060–1068. https://doi.org/10.1190/1.3640530.

Liu, S.L., Feng, J.Y., Wang, Q.Y., Su, D.W., Li, C.J., Wu, S.Q., 2019, March. Investigation on the dynamic characteristics of CG-6 relative gravimeter for the micro-gravity network. In: Tenth International Symposium on Precision Engineering Measurements and Instrumentation, vol. 11053. International Society for Optics and Photonics, p. 110531V.

Longman, I.M., 1959. Formulas for computing the tidal accelerations due to the Moon and the Sun. J. Geophys. Res. 12, 2351–2355. https://doi.org/10.1029/JZ064i012p02351.

Morales Rivera, A.M., Amelung, F., Mothes, P., Hong, S.-H., Nocquet, J.-M., Jarrin, P., 2017. Ground deformation before the 2015 eruptions of Cotopaxi volcano detected by InSAR. Geophys. Res. Lett. 44 (13), 6607–6615. https://doi.org/10.1002/2017GL073720.

Mothes, P.A., Ruiz, M.C., Viracucha, E.G., Ramón, P.A., Hernández, S., Hidalgo, S., Espín, P.A., 2017. Geophysical footprints of cotopaxi's unrest and minor eruptions in 2015: an opportunity to test scientific and community preparedness. In: Gottsmann, J., Neuberg, J., Scheu, B. (Eds.), Volcanic Unrest. Advances in Volcanology, pp. 241–270. https://doi.org/10.1007/11157_2017_10.

Petit, G., Luzum, B., 2010. IERS 2010 conventions, IERS technical note No. 36, *BKG*. Available on-line at. https://webtai.bipm.org/iers/convupdt/convupdt_c7.html.

Plouff, D., 2000. Field Estimates of Gravity Terrain Corrections and Y2K-Compatible Method to Convert from Gravity Readings with Multiple Base Stations to Tide- and Long-Term Drift-Corrected Observations. *Open-File Report* of 00-140 (available on line at pubs.usgs.gov).

Poland, M.P., de Zeeuw-van Dalfsen, E., 2019. Assessing seasonal changes in microgravity at Yellowstone caldera. J. Geophys. Res. Solid Earth 124 (4), 4174–4188. https://doi.org/10.1029/2018JB017061.

Press, W.H., Teukolsky, S.A., Vetterling, W.T., Flannery, B.P., 1992. Numerical recipes in fortran 77. Volume 1 of numerical recipes in fortran. Press syndicate of the university of cambridge. Avavilable online at. http://numerical.recipes/oldverswitcher.html.

Reudink, R., Klees, R., Francis, O., Kusche, J., Schlesinger, R., Shabanloui, A., Timmen, L., 2014. High tilt susceptibility of the Scintrex CG-5 relative gravimeters. J. Geodes. 88 (6), 617–622. https://doi.org/10.1007/s00190-014-0705-0.

Seigel, H.O., 1995. A Guide to High Precision Land Gravimeter Surveys. Scintrex Limited, Concord, Canada. Available on line at. https://scintrexltd.com/download/a-guide-to-high-precision-land-gravimeter-surveys/.

Trevino, S.F., Miller, C.A., Tikoff, B., Fournier, D., Singer, B.S., 2021. Multiple, coeval silicic magma storage domains beneath the Laguna Del Maule volcanic field inferred from gravity investigations. J. Geophys. Res. Solid Earth 126 (4), e2020JB020850. https://doi.org/10.1029/2020JB020850.

Troncoso, L., Bustillos, J., Romero, J.E., Guevara, A., Carrillo, J., Montalvo, E., Izquierdo, T., 2017. Hydrovolcanic ash emission between August 14 and 24, 2015 at Cotopaxi volcano (Ecuador): characterization and eruption mechanisms. J. Volcanol. Geoth. Res. 341, 228–241. https://doi.org/10.1016/j.jvolgeores.2017.05.032.

USNO, 2011. Selected astronomical constants, 2011. Available on line at. http://asa.usno.navy.mil/SecK/2011/Astronomical_Constants_2011.txt.

Valiant, H.D., 1991. Gravity meter calibration at LaCoste and romberg. Geophysics 56, 705–711. https://doi.org/10.1190/1.1443089.

Van Camp, M., Vauterin, P., 2005. Tsoft: graphical and interactive software for the analysis of time series and Earth tides. Comput. Geosci. 31 (5), 631–640. https://doi.org/10.1016/j.cageo.2004.11.015.

Van Camp, M., de Viron, O., Watlet, A., Meurers, B., Francis, O., Caudron, C., 2017. Geophysics from terrestrial time-variable gravity measurements. Rev. Geophys. 55 (4), 938–992. https://doi.org/10.1002/2017RG000566.